

# Link Adaptation Strategies for IEEE 802.15.4 WPANs: Protocol Design and Performance Evaluation

Youngrok Jang, Yongok Kim, Sangjoon Park, and Sooyong Choi

**Abstract:** This paper proposes two link adaptation strategies for IEEE 802.15.4 wireless personal area networks (WPANs), using a multi-rate signaling set. In the proposed link adaptation strategies, the most adequate modulation and coding scheme (MCS) satisfying the target bit error rate (BER) of the end device is selected based on the signal-to-interference-plus-noise ratio (SINR) of either a beacon or an acknowledgement (ACK) frame. The beacon-based link adaptation scheme has low complexity and overhead, given that it performs link adaptation only once per superframe. In contrast, the ACK-based strategy performs link adaptation at every ACK frame, and therefore provides a faster and more effective link adaptation, but at the expense of a larger overhead. The specific protocol design for the proposed link adaptation strategies is developed by constructing the signal flow based on the service primitives between the protocol stack layers. The network simulator OPNET is used to implement an accurate IEEE 802.15.4 WPAN protocol stack and the simulation environment required for performance evaluation. The simulation results show that the received throughput of IEEE 802.15.4 WPANs can be improved by exploiting the proposed link adaptation strategies instead of auto-rate fallback, the conventional WPAN strategy.

**Index Terms:** IEEE 802.15.4 WPANs, link adaptation, performance evaluation, protocol design, wireless sensor networks.

## I. INTRODUCTION

THE IEEE 802.15.4 wireless personal area networks (WPANs) standard [1] adopts a low-rate wireless communication protocol for low-power short-range communication systems. Recently, this standard has been widely applied as a radio access technology to smart home network systems [2]–[5], in healthcare applications [6]–[9], and to support various services based on the Internet of Things (IoT) [10]–[13].

IEEE 802.15.4 WPANs operate in the 868 MHz, 915 MHz

Manuscript received September 21, 2018; approved for publication by Lin Cai, Division II Editor, March 30, 2019.

This research was supported by the MSIT(Ministry of Science and ICT), Korea, under the ITRC(Information Technology Research Center) support program(IITP-2018-2018-0-01423) supervised by the IITP(Institute for Information & communications Technology Promotion).

Y. Jang and S. Choi are with the School of Electrical and Electronic Engineering, Yonsei University, Seoul 03722, Korea, e-mail: {dynamics, csyong}@yonsei.ac.kr.

Y. Kim is with the Network business division, Samsung Electronics Co., Ltd., 129 Samsungro, Yeongtong-gu, Suwon-si, Gyeonggi-do 16677, Korea, e-mail: yongok.kim@samsung.com.

S. Park is with the Department of Electronic Engineering, Kyonggi University, Suwon 16227, Korea, e-mail: sj.park@kgu.ac.kr.

S. Choi is the corresponding author.

Digital Object Identifier: 10.1109/JCN.2019.000027

and 2.4 GHz bands [1]. In the 2.4 GHz industrial, scientific, and medical (ISM) band, in particular, many operating devices adopt simultaneously Bluetooth with IEEE 802.15.1 [14] and IEEE 802.11 wireless local area networks (WLANs) standards [15] as communication protocols, which creates co-channel interference. Therefore, robustness against co-channel interference is an important aspect that must be considered when addressing IEEE 802.15.4 WPANs in the 2.4 GHz ISM band.

In addition, IEEE 802.15.4 WPANs operate with single data rates regardless of the operating band. However, each application supported by this standard can have a different target data rate. For example, the data frames carrying various vital signs such as electrocardiogram (ECG) and electroencephalogram (EEG) data have different target data rates depending on the healthcare applications [16]. Therefore, the flexibility to support multiple data rate should be added to IEEE 802.15.4 WPANs, so that applications with different target data rates may be supported.

To address these requirements, this paper proposes link adaptation strategies for IEEE 802.15.4 WPANs based on a multi-rate signaling set, which support multiple data rates and improve the robustness against co-channel interference. In the proposed link adaptation strategies, a modulation and coding scheme (MCS) satisfying the target bit error rate (BER) of the end device is selected based on the signal-to-interference-plus-noise ratio (SINR) of beacon or acknowledgement (ACK) frames. The beacon-based link adaptation scheme can support multiple data rates and improve robustness with low complexity and overhead, because it is executed only once for each superframe. The ACK-based link adaptation scheme, on the other hand, is executed with every ACK frame, and can therefore select a more appropriate MCS, capable of providing better robustness while supporting multiple data rates, but exhibits a larger overhead. The protocol for the proposed link adaptation strategies is designed by defining specific signal flows based on the service primitives implemented by hardware signaling between the protocol stack layers. A modified transmitter structure for applying the proposed link adaptation strategies is also developed. The performance of the proposed link adaptation strategies is evaluated by measuring various performance metrics in environments with and without WLAN interference. The proposed link adaptation strategies are compared with the conventional WLAN link adaptation strategy auto-rate fallback (ARF) [17] and with single data rate strategies, including the MCS of multi-rate signaling set and that of conventional WPANs. To create the specific simulation environments for performance evaluation, we use a network simulator to implement the protocol stack

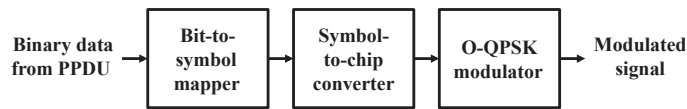


Fig. 1. Transmitter structure of the conventional IEEE 802.15.4 WPANs.

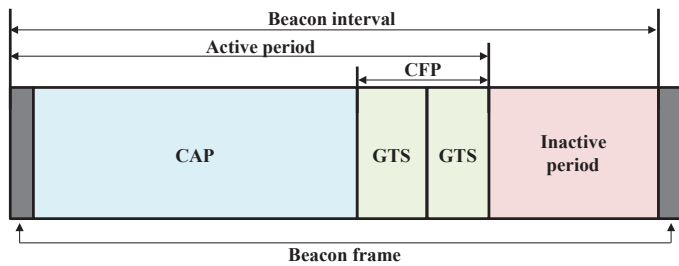


Fig. 2. Superframe structure of the conventional IEEE 802.15.4 WPANs.

of IEEE 802.15.4 WPANs and model the traffic of the WLAN interferers.

This paper is organized as follows. Section II reviews some of the approaches associated with conventional WPANs, including transmitter structure, network architecture, and the concept of service primitives. Section III introduces the proposed link adaptation strategies, including the modified transmitter structures and protocol designs for both proposed beacon-based and ACK-based link adaptation schemes. Section IV presents the performance evaluation results obtained with the network simulator OPNET. Section V concludes this paper.

## II. CONVENTIONAL WPANs

### A. Transmitter Structure

Conventional WPANs in the 2.4 GHz ISM band use direct sequence spread spectrum (DSSS)-based offset quadrature phase shift keying (O-QPSK). Fig. 1 shows the transmitter structure of conventional WPANs. Four bits from the physical protocol data unit (PPDU) are mapped into a single data symbol by the bit-to-symbol mapper, and each data symbol is mapped into a 32-chip pseudo-random noise (PN) sequence by the symbol-to-chip converter. The PN sequences of two adjacent data symbols are then jointly modulated onto a carrier using O-QPSK. Therefore, only DSSS O-QPSK with a fixed sequence length is supported, regardless of the signal-to-noise ratio (SNR). Consequently, the data rate of conventional IEEE 802.15.4 WPANs is fixed at 250 kb/s in the 2.4 GHz ISM band [1].

### B. Network Architecture

The IEEE 802.15.4 beacon-enabled WPANs operating with a star topology in the 2.4 GHz ISM band consist of a personal area network (PAN) coordinator and a number of end devices [1]. Each end device communicates only with the PAN coordinator. The medium access control (MAC) layer of IEEE 802.15.4 beacon-enabled WPANs operates using a superframe structure [1]. As shown in Fig. 2, this superframe structure consists of both an active and an inactive period. The active period is divided into the contention access period (CAP) and the

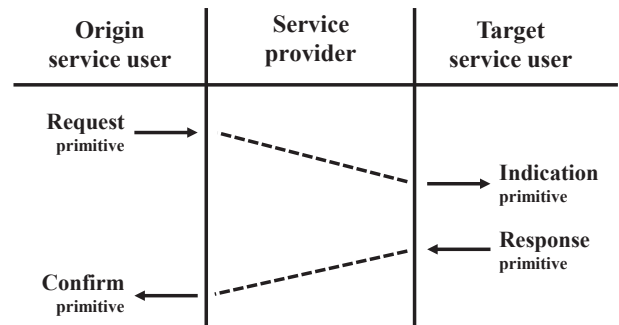


Fig. 3. Concept of service primitives.

contention free period (CFP) [1]. At the start of the active period, a beacon frame is transmitted by the PAN coordinator without using carrier sense multiple access with collision avoidance (CSMA-CA) medium access control method. The CAP period follows the beacon frame; any end devices wishing to transmit data frames should access the medium using slotted CSMA-CA during the CAP period. If present, the CFP period follows immediately after CAP, and extends to the end of the active period. During the CFP period, the scheduled end devices can be assigned to guaranteed time slots (GTS) and access the medium without contention. After the CFP, the active period terminates and an inactive period follows immediately, in which all devices turn off the transceiver and operate in low-power mode.

A number of control frames such as a beacon frame, an ACK frame, and a command frame are required to manage IEEE 802.15.4 beacon-enabled WPANs, guaranteeing the connectivity of the whole network. The beacon frame is used to synchronize the whole network and encloses the various specific control parameters for each end device. To maintain and control the full set of entities in the network, the PAN coordinator periodically transmits a beacon frame to the attached end devices. If an end device fails to receive the beacon frame for more than  $aMaxLostBeacons$  [1] consecutive times, the device loses synchronization and becomes an orphan node, which cannot communicate with the PAN coordinator. An ACK frame indicates the successful reception of the corresponding data frame. If the PAN coordinator successfully receives a data frame from an end device and the ACK request field of that data frame is set to true, the PAN coordinator transmits an ACK frame to the end device. If the number of consecutively failed ACK frames at the end device exceeds  $macMaxFrameRetries$  [1], the end device discards the corresponding data frame, clearing it from the data queue. Finally, there are various kinds of command frames in IEEE 802.15.4 WPANs, which are related to association and disassociation, data request, coordinator realignment, etc [1].

### C. Service Primitives

In this subsection, we describe the concept of *service primitives* [1], to support the explanation of the designed specific protocol. *Services* can be defined as capabilities that an arbitrary stack layer can offer to the adjacent layers. The service primitives are defined as the information signal flows occurring between the layers. Service primitives contain the information required for providing a particular service.

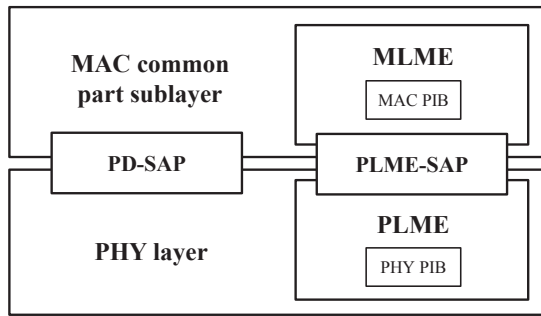


Fig. 4. Protocol stack of the IEEE 802.15.4 WPANs.

As shown in Fig. 3, there are four types of service primitives: request, indication, response, and confirm. As shown in Fig. 3, a *service provider* provides a communication path between an *origin service user* and a *target service user*. When an origin service user requires a specific service, the request primitive is issued to invoke the service and transfer the parameters needed to fully specify the requested service. The indication primitive is generated by a service provider to indicate an internal event that is significant to a target service user or is logically related to the requested service. The response and confirm primitives are specified by a target service user to complete a procedure previously invoked by the indication and request primitives, respectively, and constitute the respective acknowledgements.

To exemplify the aforementioned notion of service primitives as informational signal flows between the layers, we introduce the protocol stack of IEEE 802.15.4 WPANs comprising the PHY and MAC layers [1], as shown in Fig. 4. The PHY and MAC layers provide data and management services, respectively. The data services are provided using the PHY data (PD) service access point (SAP), which is an interface between the PHY layer and the MAC common part sublayer (MCPS). Meanwhile, the management services are provided using the PHY layer management entity (PLME) SAP, which is an interface between the PLME and the MAC layer management entity (MLME). The data and management services are supported by the related service primitives.

### III. PROPOSED LINK ADAPTATION STRATEGIES

In this section, two link adaptation strategies are proposed. One is a beacon-based link adaptation scheme and the other is an ACK-based link adaptation scheme. The modified transmitter structure necessary to support the multi-rate signaling set of the proposed schemes is explained. The specific operating procedures including the signal flow of the service primitives are also described. It is assumed that the superframe structure consists of only a CAP, and that the ACK request fields of the data frames are always set to true.

#### A. Transmitter Structure

The modified transmitter structure required to support the multi-rate signaling set for the proposed link adaptation strategies is shown in Fig. 5. Instead of the bit-to-symbol mapper and symbol-to-chip converter of the conventional DSSS trans-

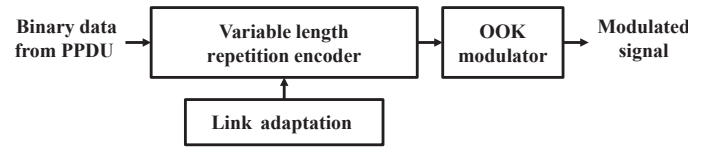


Fig. 5. Modified transmitter structure for the proposed link adaptation strategies.

Table 1. MCSs in multi-rate signaling set and conventional WPANs.

MCS index	Modulation	Repetition length	Achievable data rate (kb/s)	SNR for BER of $10^{-4}$ (dB)
1	OOK	16	62.5	0.31
2	OOK	8	125	3.33
3	OOK	4	250	6.36
4	OOK	2	500	9.39
5	OOK	1	1,000	12.42
Conventional WPANs	DSSS O-QPSK with 32-chip PN sequence		250	7.06

mitter, the modified transmitter structure uses a variable length repetition encoder, in order to support the required multiple data rate. This encoder repeats the data symbol in several time slots with a certain repetition length. If multiple data rates were to be supported using a DSSS structure with various chip rates, the system bandwidth would have to be changed for each data rate, which would imply a huge burden on the whole system. Given that the variable length repetition encoder requires the same system bandwidth for all data rates, it can be easily implemented in practice. The link adaptation block determines the length with which the variable length repetition encoder applies repetition coding to the bit stream. Repetition coding is applied here with five different lengths (1, 2, 4, 8, and 16), and therefore the multi-rate signaling set in the proposed link adaptation strategies consists of five MCSs. Then, the coded bit stream produced by the variable length repetition encoder is input to an on-off keying (OOK) modulator, given that OOK has much lower power consumption and a considerably simpler transceiver structure [19] than DSSS O-QPSK. Table 1 compares the MCSs of the proposed multi-rate signaling set and that of conventional WPANs. Basically, the BER of OOK modulation in additive white Gaussian noise (AWGN) channel based on the noncoherent detection is given by  $1/2 \exp(-\gamma/2)$  as in [20], where  $\exp(\cdot)$  and  $\gamma$  denote the exponential function and SNR, respectively. Therefore, in order to achieve BER of  $10^{-4}$ , the required SNR for the OOK modulation without repetition coding, i.e., the MCS 5, is 12.42 dB. Further, by exploiting 1 MHz of system bandwidth, the achievable data rate of the OOK modulation without repetition coding, i.e., the MCS 5, is 1 Mb/s. Then, if the MCS index decreases by one step, the length of the repetition coding is doubled and therefore the 3 dB of an additional processing gain is achieved. Instead, the achievable data rate is halved. For example, if the MCS index is changed from 5 to 4, the achievable data rate decreases from 1 Mb/s to 500 kb/s and the required SNR to achieve BER of  $10^{-4}$  decreases from 12.42 dB to 9.39 dB. Therefore, for the case of the MCS 3, the achievable data rate and the required SNR can be calculated as

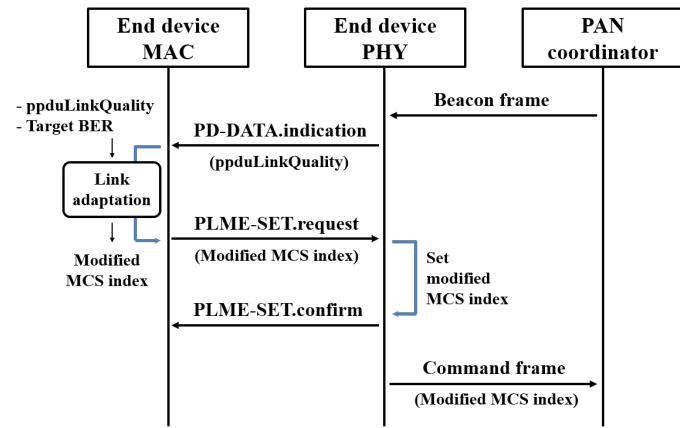


Fig. 6. Signal flow between the protocol stacks for the proposed beacon-based link adaptation scheme.

250 kb/s and 6.36 dB, respectively. Note that the proposed link adaptation strategies are applied to the data frames only.

**B. Beacon-Based Link Adaptation Scheme**

The signal flow of the proposed beacon-based link adaptation scheme is based on the standard protocol stack of IEEE 802.15.4 WPANs [1], and is shown in Fig. 6. When the PAN coordinator transmits a beacon frame, the PHY layer of each end device receiving the beacon frame measures the signal-to-interference-plus-noise ratio (SINR) of the received beacon frame by using the receiver energy detection (ED) [1] and calculates the *ppduLinkQuality* [1] parameter by quantizing the measured SINR. After the calculation, the PHY layer generates the PD-DATA.indication primitive [1], which contains the *ppduLinkQuality* of the received beacon frame and sends it to the MAC layer. In the MAC layer, the proposed beacon-based link adaptation scheme is performed using the following two quantities: 1) The *ppduLinkQuality*, which indicates the approximate SINR of the beacon frame, and 2) the target BER which can be defined by the application being used at each end device. For a given SINR, as provided by the *ppduLinkQuality* parameter, the link adaptation block in the MAC layer chooses the MCS index that satisfies the target BER with the shortest repetition length. The MAC layer then generates the PLME-SET.request primitive [1], which contains the modified MCS index, and sends it back to the PHY layer. After setting the modified MCS index, the PHY layer generates and delivers the PLME-SET.confirm primitive [1] to the MAC layer. Finally, to inform the PAN coordinator of the selected repetition length, each end device transmits a predefined command frame containing the modified MCS index. After receiving the command frame, the PAN coordinator can be informed which MCS index is applied to the data frame of each end device and conduct the suitable receiving scheme for the corresponding modified MCS index. The end device then transmits its data frames using the selected MCS index until receiving the next beacon frame.

Given that the beacon frame must be sufficiently robust to reach and maintain synchronization through the whole network, it is encoded with the maximum repetition coding length, 16. Like as the beacon frame, the command frame is also encoded

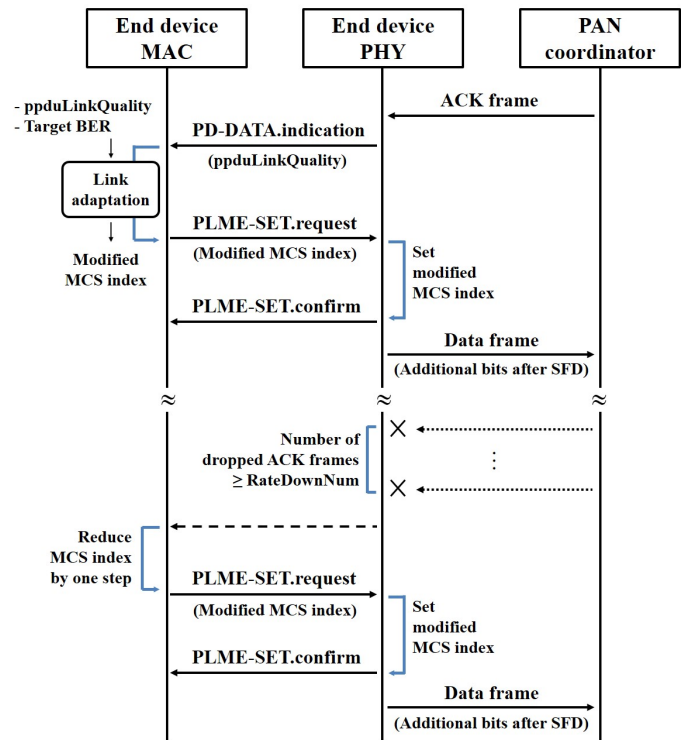


Fig. 7. Signal flow between the protocol stacks for the proposed ACK-based link adaptation scheme.

by the same repetition length, i.e., MCS 1, in order to inform the modified MCS index definitely. Additionally, the fact that the PAN coordinator and the end devices have different transmit power levels must be taken into account. Therefore, the power offset, according to the processing gain of the repetition coding, and the different transmit power levels should be considered in the calculations of the SINR value and the corresponding repetition length.

In summary, based on the SINR of the beacon frame and the target BER of each end device, the proposed beacon-based link adaptation scheme selects the most suitable MCS index at every beacon frame. The end device then uses that MCS index during the superframe, until the arrival of the next beacon frame. If a beacon frame is dropped because of a poor channel state or collision with other packets, the end device reutilizes the previously chosen MCS index to transmit its data frames. The beacon-based link adaptation scheme can be easily applied with low signaling overhead, because the MCS of each end device can only change with beacon frames and is maintained constant during the corresponding superframes.

**C. ACK-Based Link Adaptation Scheme**

The signal flow of the proposed ACK-based link adaptation scheme is shown in Fig. 7. When the PAN coordinator transmits an ACK frame to the end device (in response to a data frame), the PHY layer of the end device receiving the ACK frame measures the SINR of the ACK frame and calculates the *ppduLinkQuality* parameter by quantizing the measured SINR, as before. The PHY layer then generates a PD-DATA.indication primitive, which contains the *ppduLinkQuality* of the received

ACK frame, and sends it to the MAC layer. In the MAC layer, using the `ppduLinkQuality` and the target BER of the end device, the link adaptation block chooses the smallest MCS index satisfying the target BER and transfers it to the PHY layer with the `PLME-SET.request` primitive. After setting the modified MCS index, the PHY layer generates and delivers a `PLME-SET.confirm` primitive to the MAC layer, and the end device transmits a data frame to the PAN coordinator.

As shown in Figs. 6 and 7, the proposed ACK-based link adaptation scheme has a signal flow similar that of the beacon-based link adaptation scheme. However, in the ACK-based link adaptation scheme, a `RateDownNum` parameter is additionally defined, to deal with the case of dropped ACK frames. While the number of consecutively failed ACK frames is lower than `RateDownNum`, the end device reutilizes the previously chosen MCS index to retransmit the data frame. On the other hand, when the number of consecutively failed ACK frames reaches above `RateDownNum`, the end device reduces the MCS index by one. Therefore, instead of always using the previously chosen MCS index, as in the beacon-based link adaptation scheme, the ACK-based link adaptation scheme can adjust the MCS index during the superframe.

Since ACK frames are much more frequent than beacon frames [1], sending a command frame as feedback of the MCS choice made at every ACK frame would lead to a significant overhead. Therefore, in the proposed ACK-based link adaptation scheme, the data frame MCS index is carried by additional bits following the start-of-frame delimiter (SFD) field in the data frame synchronization header [1], and not with a command frame as in the beacon-based link adaptation scheme. Since there are five MCSs in the multi-rate signaling set, additional 3 bits are required to represent the MCS index.

As discussed above, the proposed ACK-based link adaptation scheme selects the most suitable MCS index at every ACK frame, based on the ACK frame SINR and the target BER of each end device. Since ACK frames are much more frequent than beacon frames [1], the ACK-based link adaptation scheme has a much shorter link adaptation period than the beacon-based link adaptation scheme. Furthermore, unlike the beacon-based link adaptation scheme, the ACK-based link adaptation scheme can adjust the MCS index during the superframe. Therefore, the ACK-based link adaptation scheme can reflect the quality of the communication links more accurately than the beacon-based link adaptation scheme. However, the signal flow in Fig. 7 is generated by every received ACK frame for the ACK-based link adaptation scheme, which is more frequent than the beacon-based link adaptation scheme which the signal flow in Fig. 6 is generated once during each superframe. Hence, the beacon-based link adaptation scheme can require a lower power consumption than the ACK-based one.

#### IV. PERFORMANCE EVALUATION OF THE PROPOSED LINK ADAPTATION STRATEGIES

The simulation environment for performance evaluation considers a topology with three WPAN end devices, one PAN coordinator, and one WLAN interferer, as shown in Fig. 8. The PAN coordinator is at 2 m and 40 m from the end devices and the in-

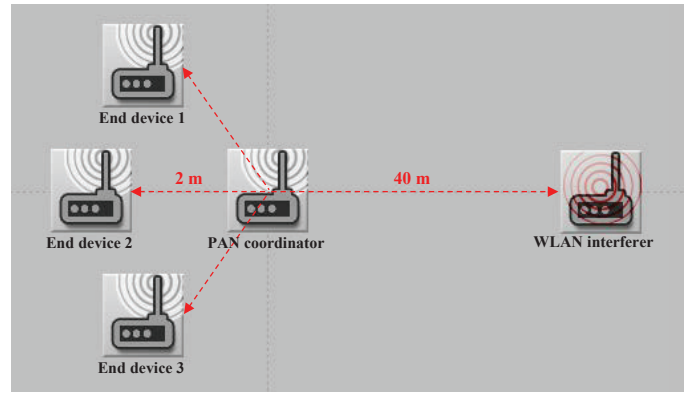


Fig. 8. Simulation environment topology with WPAN end devices, a PAN coordinator, and a WLAN interferer.

Table 2. System parameters of each device type for simulations.

Device type	System parameters	Value
WPAN end device (Full buffer model)	Transmit power	0 dBm
	Packet length	512 bits
	Target BER	$10^{-4}$
	RateDownNum	3
WPAN coordinator	Transmit power	10 dBm
	Beacon order	6
	Superframe order	3
	System bandwidth	1 MHz
	Center frequency	2.410 GHz
WLAN interferer	Transmit power	20 dBm
	Packet length	2048 Bytes
	Data rate	54 Mb/s
	System bandwidth	22 MHz
	Center frequency	2.412 GHz

terferer, as shown in Fig. 8. The end devices transmit their data frames to the PAN coordinator using CSMA-CA. The parameters of the WPAN end devices, PAN coordinator, and WLAN interferer are shown in Table 2. Two simulation scenarios are examined: 1) IEEE 802.15.4 WPAN without an interfering IEEE 802.11 WLAN [21], [22] and 2) IEEE 802.15.4 WPAN with an interfering IEEE 802.11 WLAN [23]. That is, in Scenario 1), the WLAN interferer is deactivated.

The large scale fading of each communication link is generated using the path loss model [24] given by

$$P_L(d) = 20 \log_{10} \left( \frac{4\pi d}{\lambda} \right) + L_w(d-4)u(d-4), \quad (1)$$

where  $d$  and  $\lambda$  are the transmitter-receiver distance and the carrier wavelength, respectively, and  $u(\cdot)$  is the unit step function (1 for nonnegative arguments, and 0 otherwise).  $L_w$  is an additional path loss beyond 4 meters which is considered to be 0.7 dB/m for an indoor scenario [24]. The small scale fading channel coefficients are maintained constant over one frame duration and may vary between successive frames [25]. The channel coefficient of each frame is correlated with that of the previous frame as follows:

$$h_k = \alpha h_{k-1} + \sqrt{1 - \alpha^2} z, \quad (2)$$

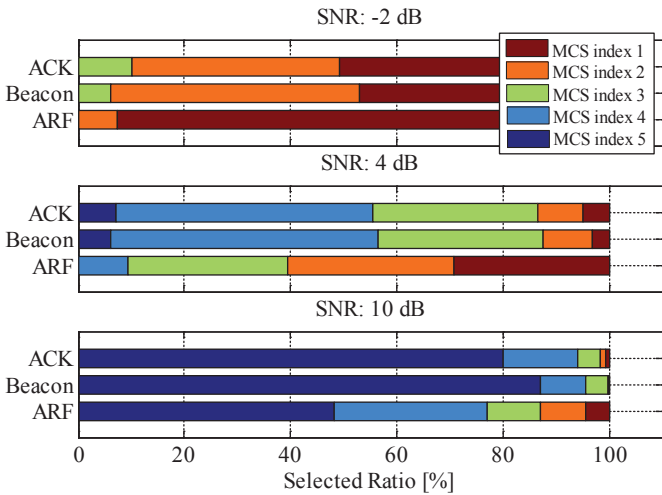


Fig. 9. Selection ratio of the ARF, the beacon-based link adaptation scheme, and the ACK-based link adaptation scheme according to the average received SNR without the WLAN interferer.

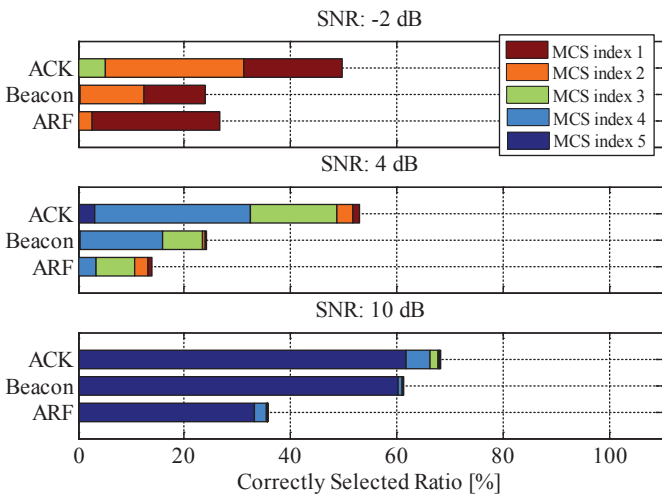


Fig. 10. Correct selection ratio of the ARF, the beacon-based link adaptation scheme, and the ACK-based link adaptation scheme according to the average received SNR without the WLAN interferer.

where  $h_{k-1}$  and  $h_k$  are the channel coefficients of the previous and current frames, respectively. The random variable  $z$  is the innovation process which is considered to follow an independent and identically distributed (i.i.d) complex Gaussian distribution with zero mean and unit variance [26]. The temporal correlation coefficient  $\alpha$ , which represents the degree of correlation between  $h_{k-1}$  and  $h_k$  is set to 0.8 [25].

The performance of the proposed link adaptation strategies is compared with those of ARF [17] applied to WPANs. As mentioned above, ARF is the link adaptation strategy of IEEE 802.11 WLANs. It changes the data rate of a WLAN node based on the number of successfully received or failed ACK frames. If an end device successfully receives 10 consecutive ACK frames, it increases the data rate by one step. On the other hand, if an end device fails to receive 3 consecutive ACK frames, it decreases the data rate by one step. Furthermore, the performance of single data rate strategies such as DSSS O-QPSK (the con-

ventional WPAN scheme at 2.4 GHz) and each of the MCSs in Table 1 are also evaluated. The evaluation uses the performance metrics that can be obtained from the PHY and MAC layers. For an accurate implementation of the IEEE 802.15.4 standard, the network simulator OPNET (modeler version 17.5) is used to construct the specific simulation environments, such as the entire protocol stack of IEEE 802.15.4 WPANs, the signal flows of the different service primitives, the traffic modeling at each node, and the network topologies. A new control overhead is also constructed and considered in the simulation, i.e., a command frame containing the modified MCS index for the beacon-based link adaptation scheme and additional bits representing the modified MCS index after SFD for the ACK-based link adaptation scheme. However, since only a single command frame for the beacon-based link adaptation scheme is additionally transmitted for every superframe and additional 3 bits is significantly smaller than the length of the data frame, i.e., 512 bits as shown in Table 2, the effect of a new control overhead can be neglected for both two proposed schemes. The simulation results are obtained from 100 iterations with different random seeds; almost 10,000,000 discrete events are generated at each iteration.

A. Performance of the WPAN without WLAN Interference

In this subsection, the performance of the WPAN without the WLAN interference is evaluated. The performance metrics are based on the uplink data transmission, as measured at PAN coordinator’s receiver.

Figs. 9 and 10 show the ratios of the selected indexes, respectively, for the evaluated link adaptation strategies; these ratios are shown for different average SNRs at the PAN coordinator’s receiver. The selection ratio of the link adaptation strategy represents simply the frequency with which the several MCSs are selected. The correct selection ratio represents the probability that the link adaptation strategy chooses the smallest MCS index among the MCS indexes satisfying the target BER for each received frame; that is, the MCS index satisfying the target BER with the maximum achievable data rate. Given the importance of choosing the most adequate MCS index, the correct selection ratio is an important indicator to determine a good link adaptation strategy.

As shown in Fig. 9, ARF usually selects the MCS with the longest or shortest repetition length at low or high received SNRs, respectively. This is because ARF changes the MCS index when a particular number of consecutive ACK frames are either successfully received or lost. Moreover, the ARF changes MCS by only one step at a time. Therefore, it shows a lower correct selection ratio than the ACK-based link adaptation scheme. On the other hand, the beacon-based link adaptation shows a lower correct selection ratio than ARF in the low SNR region, because it uses the same MCS during the superframe. However, given that the beacon-based link adaptation scheme can change the MCS in arbitrary steps according to the received SINR of the beacon frame, it achieves a higher correct selection ratio than ARF as the average received SNR increases. The ACK-based link adaptation scheme can also change the MCS in arbitrary steps according to the received SINR of ACK frames, and can do so during the superframe. Therefore, it achieves a signifi-

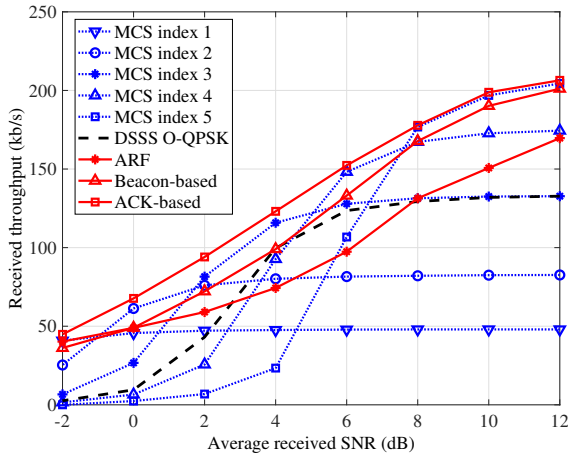


Fig. 11. Received throughput at the PAN coordinator according to the average received SNR.

cantly higher correct selection ratio than both the beacon-based link adaptation scheme and ARF, regardless of the average received SNR.

Fig. 11 shows the received throughputs at the PAN coordinator as a function of the average received SNR. As shown, the received throughput of each single data rate strategy saturates after a certain SNR value, because of the fixed modulation and repetition length of single data rate strategies. The saturation values are slightly different from the achievable data rates shown in Table 1, because the existing additional redundancies, such as the command frame and the header and cyclic redundancy check of each frame, are also being considered in Fig. 11. It can be further noted that the MCS index 3 has better performance than the DSSS O-QPSK (of the conventional WPANs) since the required SNR of the MCS index 3 achieving BER of  $10^{-4}$  is smaller than that of the DSSS O-QPSK, as shown in Table 1. In other words, the error performance of the MCS index 3 is better than that of the DSSS O-QPSK. However, since achievable data rates and error performances of both the MCS index 3 and DSSS O-QPSK are similar as shown in Table 1, two schemes achieve almost same received throughput at high SNR region. Meanwhile, the ACK-based link adaptation scheme outperforms the other link adaptation strategies and/or single data rate strategies in terms of received throughputs. As shown in Fig. 10, when the SNR is  $-2$  or  $4$  dB, various MCS indexes can be correctly selected by using the ACK-based link adaptation scheme. Hence, the ACK-based link adaptation scheme can outperform all the single data rate strategies at low SNR region as shown in Fig. 11. However, when the SNR is  $10$  dB in Fig. 10, the correct selection ratio of the MCS index 5 is significantly higher than those of the other MCS indexes by using the ACK-based link adaptation scheme. Therefore, the performance gap between the ACK-based link adaptation scheme and the MCS index 5 can decrease at high SNR region. Although the ARF shows higher received throughputs than the beacon-based link adaptation scheme in the low SNR region, the beacon-based link adaptation scheme outperforms the ARF as the average received SNR increases.

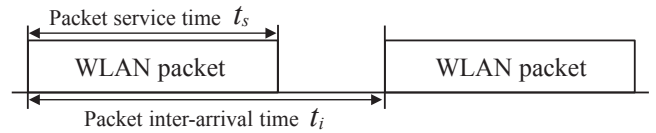


Fig. 12. Duty cycle modeling by using the packet service time and the packet inter-arrival time of the WLAN interferer.

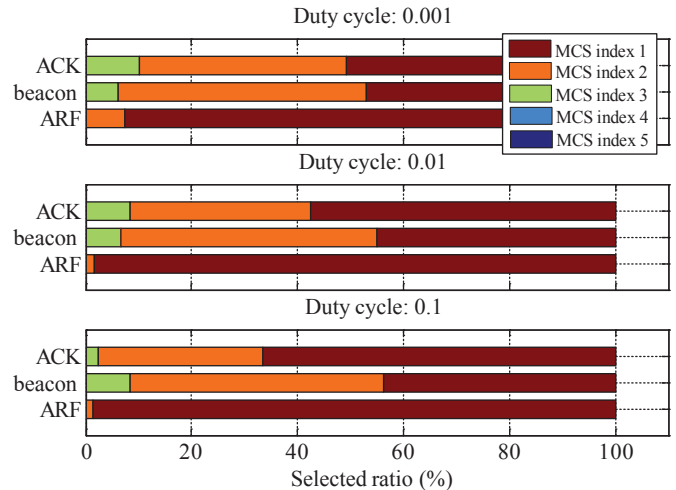


Fig. 13. Selection ratio of the ARF, the beacon-based link adaptation scheme, and the ACK-based link adaptation scheme according to the duty cycle of the WLAN interferer.

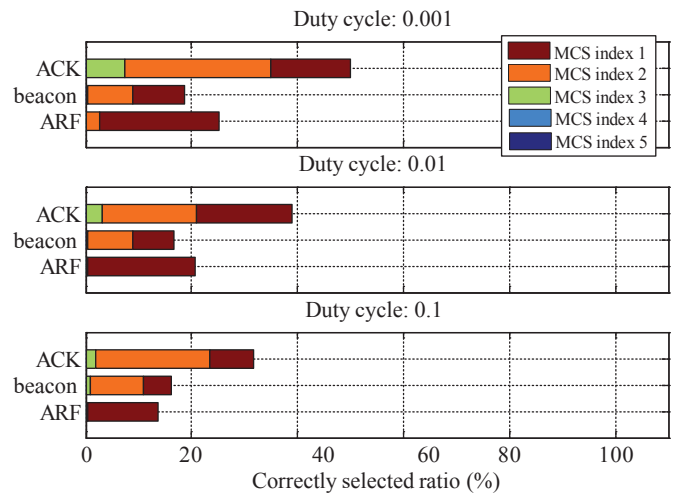


Fig. 14. Correct selection ratio of the ARF, the beacon-based link adaptation scheme, and the ACK-based link adaptation scheme according to the duty cycle of the WLAN interferer.

### B. Performance of WPAN with WLAN Interference

In this subsection, the WPAN performance is evaluated when an interfering WLAN is present. As shown in Table 2, the center frequency of the WLAN is considered to be  $2.412$  GHz, which corresponds to Channel 1 of the North American channel selection model [15]. It is assumed that the WPAN end devices execute the CSMA-CA protocol without considering the existence of the WLAN interferer. The data rate of the WLAN interferer is set to  $54$  Mb/s [15]. Therefore, the duration of the

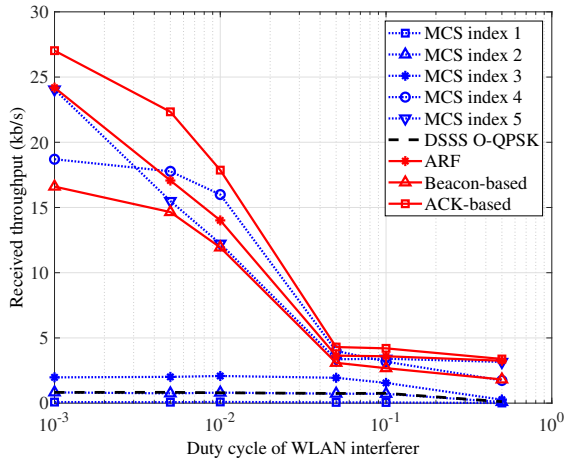


Fig. 15. Received throughput at the PAN coordinator according to the duty cycle of the WLAN interferer.

WLAN packet is shorter than that of the WPAN packet. The traffic pattern of the WLAN interferer is modeled using its duty cycle [25]. As shown in Fig. 12,  $t_s$  and  $t_i$  denote the packet service time and packet inter-arrival time, respectively. The duty cycle is then defined as the ratio of the packet service time to the packet inter-arrival time ( $t_s/t_i$ ). Given that a constant WLAN packet length is assumed, the duty cycle increases as the packet inter-arrival time of the WLAN interferer decreases.

The selection ratio and correct selection ratio of the link adaptation strategies in the presence of the WLAN interferer are shown in Figs. 13 and 14, respectively. The average received SNR at the PAN coordinator without WLAN interference is set to  $-2$  dB. The considered duty cycle is a measure of the packet transmission rate of the WLAN interferer. Therefore, as the duty cycle decreases, the overall amount of interference from the WLAN packets on the WPAN end device receivers decreases, and the instantaneous SNRs and SINRs become similar. Therefore, for low duty cycles, similar results to those of in Figs. 9 and 10, ARF outperforms the beacon-based link adaptation scheme in terms of the correct selection ratio. However, as the duty cycle increases, the probability of successfully receiving 10 consecutive ACK frames decreases, since the instantaneous SINR of the ACK frames is significantly degraded by interference from the WLAN packets. Consequently, the ARF tends to select MCS index 1 as the duty cycle increases, and the beacon-based link adaptation scheme achieves a higher correct selection ratio than ARF for the high (0.1) duty cycle. Meanwhile, similarly to what was observed in Figs. 9 and 10, the ACK-based link adaptation scheme shows the highest correct selection ratio, regardless of duty cycle, because of its fast link adaptation speed and the ability to change MCS in arbitrary steps.

Fig. 15 shows the received throughputs at the PAN coordinator as a function of the WLAN interferer duty cycle. For all strategies, the received throughput saturates after a duty cycle of 0.05, because of the large amount of interference. Further, the MCSs with high data rates, MCS indexes 4 and 5, show significantly low received throughputs (close to 0) because of the low average received SNRs and the presence of the WLAN

interferer. Meanwhile, although the performance gap between the ACK-based link adaptation scheme and ARF almost vanishes for duty cycles above 0.05, the ACK-based link adaptation scheme outperforms the other link adaptation strategies and the single data rate strategies in terms of received throughput, similarly to what was observed in the case where no WLAN interferer was present (Fig. 11).

It can also be observed in Fig. 15 that MCS index 1, with the longest repetition length, can have lower received throughputs than MCS index 2. The reason is that MCS index 1 has a frame duration twice as long as that of MCS index 2, and therefore experiences more collisions with WLAN packets. Therefore, shortening the frame duration can reduce the possibility of collisions with the WLAN packets and results in an improved throughput at duty cycles close to 0.01, as shown in Fig. 15. This phenomenon is not observed for low or high duty cycles, because in those situations the number of collisions with the WLAN packets is either very small or large, respectively, regardless of the frame duration. Therefore, a best repetition length exists for a particular duty cycle of the WLAN interferer. Given that the proposed ACK-based link adaptation strategy can rapidly change to the most adequate MCS level, reflecting the channel link conditions, it achieves a better performance than the other link adaptation schemes and single data rate strategies with respect to received throughput.

## V. CONCLUSION

In this paper, two link adaptation strategies for IEEE 802.15.4 WPANs were proposed. Based on a multi-rate set and a modified transmitter structure adequate for easy link adaptation, the proposed link adaptation strategies use the information obtained from the received beacon or ACK frames. Despite its low complexity and overhead, the beacon-based link adaptation scheme can support multiple data rates and achieve improved robustness to co-channel interference. The ACK-based link adaptation scheme, on the other hand, by adapting at every ACK frame, can quickly select the MCS most adequate to improve robustness while supporting multiple data rates, but requires a large overhead. The specific protocol design was based on the signal flow of service primitives between the PHY and MAC layers. The performance of the proposed link adaptation strategies was evaluated and compared with ARF (applied to WPAN) and to single data rate strategies (including that of conventional WPANs). Accurate protocol-level simulations were performed with the network simulator OPNET. The performance evaluation results show that the proposed ACK-based link adaptation scheme has the highest correct MCS selection ratio among the considered link adaptation strategies and outperforms all the other strategies in terms of received throughput, regardless of the presence of WLAN interference. Therefore, the proposed ACK-based link adaptation scheme can provide increased robustness against co-channel interference and multiple data rates to the various applications on IEEE 802.15.4 WPANs.

## REFERENCES

- [1] Approved IEEE draft amendment to IEEE standard for information technology-telecommunications and information exchange between



systems-Part 15.4: Wireless medium access control (MAC) and physical layer (PHY) specifications for low-rate wireless personal area networks (LR-WPANS): Amendment to add alternative Phy, IEEE Std. 802.15.4, 2007.

- [2] C. Gomez and J. Paradells, "Wireless home automation networks: A survey of architectures and technologies," *IEEE Commun. Mag.*, vol. 48, no. 6, pp. 92–101, May 2010.
- [3] J. Han, C. Choi, W. Park, I. Lee and S. Kim, "Smart home energy management system including renewable energy based on ZigBee and PLC," *IEEE Trans. Consum. Electron.*, vol. 60, no. 2, pp. 198–202, May 2014.
- [4] J. Han *et al.*, "Smart home energy management system including renewable energy based on ZigBee and PLC," *IEEE Trans. Consum. Electron.*, vol. 60, no. 3, pp 198–202, June 2014.
- [5] E. Spanò, S. Di Pascoli, and G. Iannaccone, "Low-power wearable ECG monitoring system for multiple-patient remote monitoring," *IEEE Sensors J.*, vol. 16, no. 13, pp 5452–5462, July 2016.
- [6] S. Ullah *et al.*, "A comprehensive survey of wireless body area networks," *J. Medical Systems*, vol. 36, no. 3, pp. 1065–1094, Aug. 2010.
- [7] M. Deylami, and E. Jovanov, "A distributed scheme for managing the dynamic coexistence of IEEE 802.15.4-based health monitoring WBANs," *IEEE J. Biomed. Health Inf.*, vol. 18, no. 1, pp. 327–334, Jan. 2014.
- [8] J. Gil *et al.*, "A fully integrated low-power high-coexistence 2.4-GHz Zig-Bee transceiver for biomedical and healthcare applications," *IEEE Trans. Microw. Theory Techn.*, vol. 62, no. 9, pp. 1879–1889, Sept. 2014.
- [9] M. Pavana *et al.*, "System architecture for low-power ubiquitously connected remote health monitoring applications with smart transmission mechanism," *IEEE Sensors J.*, vol. 15, no. 8, pp. 4532–4543, Aug. 2015.
- [10] Y. Liu and G. Zhou, "Key technologies and applications of internet of things," in *Proc. IEEE ICICTA*, Jan. 2012, pp. 197–200.
- [11] M. R. Palattella *et al.*, "Standardized protocol stack for the internet of (important) things," *IEEE Commun. Surveys Tuts.*, vol. 15, no. 3, pp. 1389–1406, 3rd Quart. 2013.
- [12] M. Hassanaliyagh *et al.*, "Health monitoring and management using internet-of-thing sensing with cloud-based processing - opportunities and challenges," *Proc. IEEE SCC*, June 2015, pp. 285–292.
- [13] C.-S. P, "A secure and efficient ECQV implicit certificate issuance protocol for the internet of things applications," *IEEE Sensors J.*, vol. 17, no. 7, pp. 2215–2223, Apr. 2017.
- [14] Part 15.1: Wireless medium access control (MAC) and physical layer (PHY) specifications for wireless personal area networks (WPANS), IEEE Std. 802.15.1, 2005.
- [15] Part 11: Wireless medium access control (MAC) and physical layer (PHY) specifications, IEEE Std. 802.11, 2007.
- [16] D. Raskovic *et al.*, "From telemedicine to ubiquitous M-Health: The evolution of E-Health systems," *Biomed. Inform. Tech.*, Academic Press, pp. 479–496, 2008.
- [17] A. Kamerman and L. Monteban, "WaveLAN-II: a high-performance wireless LAN for the unlicensed band," *Bell Labs Tech. J.*, vol. 2, no. 2, pp. 118–133, 1997.
- [18] Y. Jang, Y. Kim, and S. Choi, "Link adaptation strategy for healthcare application on IEEE 802.15.4 WPANs," in *Proc. IEEE ICCE*, Las Vegas, USA, Jan. 2015, pp. 248–249.
- [19] J. Polastre, R. Szwedczyk, and D. Culler, "TELOS: enabling ultra-low power wireless research," in *Proc. IEEE IPSN*, Apr. 2005, pp. 364–369.
- [20] M. Schwartz, W. R. Bennett, and S. Stein, *Communication Systems and Techniques*, McGraw-Hill, 1966.
- [21] J.-S. Lee, "Performance evaluation of IEEE 802.15.4 for low-rate wireless personal area networks," *IEEE Trans. Consum. Electron.*, vol. 52, no. 3, pp. 742–749, Aug. 2006.
- [22] C.-S. Sum *et al.*, "Error performance and throughput evaluation of a multi-Gbps millimeter-wave WPAN system in the presence of adjacent and co-channel interference," *IEEE J. Sel. Areas Commun.*, vol. 27, no. 8, pp. 1433–1442, Oct. 2009.
- [23] S. Y. Shin, H. S. Park, and W. H. Kwon, "Mutual interference analysis of IEEE 802.15.4 and IEEE 802.11b," *Comput. Netw.*, vol. 51, no. 12, pp. 3338–3353, Aug. 2007.
- [24] A. Petroff and K. Siwiak, "A path link model for ultra wide band pulse transmissions," in *Proc. IEEE VTC*, New Jersey, USA, May 2001, pp. 1173–1175.
- [25] R. R. Rout and S. K. Ghosh, "Enhancement of lifetime using duty cycle and network coding in wireless sensor networks," *IEEE Trans. Wireless Commun.*, vol. 12, no. 2, pp. 656–667, Feb. 2013.
- [26] T. S. Rappaport, *Wireless Communications*. Englewood Cliffs, NJ: Prentice-Hall, 1996.



**Youngrok Jang** was born in Seoul, Korea, in 1989. He received the B.S. degree in electrical and Electronic Engineering from Yonsei University, Seoul, Korea, in 2012. He is currently working toward the Ph.D. degree at the same university. His primary research interests include ultra-low power wireless sensor networks (e.g., IEEE 802.15.4 WPANs), in-band full-duplex wireless systems, FDD massive MIMO systems, advanced CSI feedback scheme for 3GPP NR, SWIPT systems, and machine learning based wireless communication systems.



**Yongok Kim** received the B.S. and Ph.D. degrees in Electrical and Electronic Engineering from Yonsei University, Seoul, Korea in 2010 and 2016, respectively. Since March 2016, he has been with Samsung Electronics Co., Ltd., Suwon, Korea as a Senior Engineer. His current research interests include massive MIMO/beamforming systems and 5G mobile communication systems.



**Sangjoon Park** was born in Seoul, Korea, in 1981. He received the B.S., M.S., and Ph.D. degrees in Electrical and Electronic Engineering from Yonsei University, Seoul, Korea, in 2004, 2006, and 2011, respectively. From August 2011 to February 2014, he was with LG Electronics, as a Senior Research Engineer participating in research about telematics and vehicular communication systems. From April 2014 to August 2016, he was a Research Professor with the School of Electrical and Electronic Engineering, Yonsei University. From September 2016 to February 2019, he was an Assistant Professor with the Department of Information and Communication Engineering, Wonkwang University. From March 2019, he has been an Assistant Professor with the Department of Electronic Engineering, Kyonggi University, Suwon, Korea. His main research interests include communication signal processing techniques, such as detection and equalization algorithms, hybrid ARQ and MIMO applications for wireless communications, error correcting codes, algorithms for physical layer security, and other signal processing techniques.



**Sooyong Choi** was born in Seoul, South Korea, in 1971. He received the B.S.E.E., M.S.E.E., and Ph.D. degrees from Yonsei University, Seoul, in 1995, 1997, and 2001, respectively. In 2001, he was a Post-Doctoral Researcher with the IT Research Group, Yonsei University. His work focused on proposing and planning for the fourth generation communication system. From 2002 to 2004, he was a Post-Doctoral Fellow with the University of California at San Diego, La Jolla, CA, USA. From 2004 to 2005, he was a Researcher with Oklahoma State University, Stillwater, OK, USA. From 2005 to 2016, he was Assistant Professor and Associate Professor with the School of Electrical and Electronic Engineering, Yonsei University. Since 2016, he has been a Professor with the School of Electrical and Electronic Engineering. His research interests include adaptive signal processing techniques (equalization and detection), massive MIMO systems for wireless communication, and new waveforms and multicarrier transmission techniques for future wireless communication systems.